Am J Cancer Res 2025;15(1):113-126
www.ajcr.us /ISSN:2156-6976/ajcr0161783

Original Article

Identification of sinensetin as a selective inhibitor for mitogen-activated protein kinase kinase 6 and an anticancer agent for non-small cell lung cancer

Xiaomeng Xie[1,2,3*], Young Ran Shin[4,5*], Tae-Sung Kim[5,6*], Yeon-Sun Seong[5,6], Yong Weon Yi[5,6], Dong Joon Kim[2,3,4,5]

[1]Chest Hospital of Zhengzhou University, Zhengzhou 450000, Henan, China; [2]Department of Pathophysiology, School of Basic Medical Sciences, Academy of Medical Science, College of Medicine, Zhengzhou University, Zhengzhou 450008, Henan, China; [3]China-US (Henan) Hormel Cancer Institute, Zhengzhou 450008, Henan, China; [4]Department of Microbiology, College of Medicine, Dankook University, Cheonan-si 31116, Chungcheongnam-do, Republic of Korea; [5]Multidrug-Resistant Refractory Cancer Convergence Research Center (MRCRC), Dankook University, Cheonan-si 31116, Chungcheongnam-do, Republic of Korea; [6]Department of Biochemistry, College of Medicine, Dankook University, Cheonan-si 31116, Chungcheongnam-do, Republic of Korea. [*]Equal contributors.

Received November 6, 2024; Accepted January 3, 2025; Epub January 15, 2025; Published January 30, 2025

Abstract: Natural compounds are an invaluable source for bioactive small molecules. Cellular activities modulated by them are generally achieved by binding specific cellular targets. However, identification of target(s) for a natural compound is challenging and a hurdle for further development of them as drugs. Sinensetin is derived from *Schisandra sphenanthera* and the major component of a traditional medicine. Although Sinensetin possesses pharmacological activities, including antioxidants, anti-inflammatory, and anticancer, the molecular mechanisms for its activities remain unclear due to lack of information for its target. In addition, the anticancer effects of sinensetin against non-small cell lung cancer (NSCLC) have not been studied. Here, we described sinensetin as a specific inhibitor of MKK6 with a KD value of 66.27 μM. Sinensetin inhibited the proliferation of NSCLC cells and lung patient-derived xenograft-derived organoids (LPDXO), and induced G1 phase cell-cycle arrest. Sinensetin attenuated the MAPK signaling pathway by directly inhibiting MKK6, but not MKK3. *In silico* molecular docking analysis indicated that sinensetin was specifically bound near the αG-helix of MKK6, but not MKK3. High MKK6 expression levels were observed in NSCLC patients. MKK6 knockout abolished the sinensetin-mediated inhibition of NSCLC cell proliferation. Taken together, sinensetin is a novel MKK6 inhibitor with therapeutic potential for NSCLC.

Keywords: Sinensetin, lung patient-derived xenograft-derived organoids, non-small cell lung cancer, MKK6, p38α, MKK3, *in silico*, cancer growth, novel inhibitor, cell cycle

Introduction

Natural products have long served as a major source of pharmacotherapy and were recently revitalized as a source of lead compounds with advancements in technologies and scientific knowledge [1, 2]. However, target identification (ID) of natural products and their derivatives remains a major hurdle in drug development. Without target ID, it is difficult to elucidate the mode of action of natural products and optimize their cellular activities [1, 2].

Prior to the establishment of modern medicine, traditional medicine, rooted in the geographical diversity of soil and traditional ethnic foods, was closely tied to medicine and life through empirical prescriptions. This foundation significantly contributed to the development of modern pharmaceuticals. Zhuang medicine, a form of traditional Chinese medicine, has been used clinically and exhibits anti-inflammatory effects [3]. Sinensetin, the main component of Zhuang medicine, is a plant-derived polymethoxylated flavonoid found in *Orthosiphon aristatus* var. *aristatus* that has been used in traditional folk medicine [4-7]. It exhibits anti-oxidant, anti-inflammatory [8], anti-microbial, anti-obesity, anti-dementia, and vasorelaxant activities [9]. Sinensetin attenuates IL-1β-induced cartilage

damage and ameliorates osteoarthritis by regulating α-1-antichymotrypsin serpin family A member 3 (SERPINA3) levels [10]. Moreover, it induces autophagic cell death through p53-related AMP-activated kinase (AMPK)/mammalian target of rapamycin (mTOR) signaling in HepG2 hepatocellular carcinoma cells [11]. Additionally, sinensetin suppresses angiogenesis in liver cancer by targeting the vascular endothelial growth factor (VEGF)/VEGF receptor 2 (VEGFR2)/AKT signaling pathway [12]. However, cellular targets for sinensetin have not been identified yet.

MAPK signaling pathways play a key role in cell proliferation, survival, and invasion [13]. The MKK3/6-p38 signaling pathway is a key MAPK signaling pathway involved in various pathologies, including inflammation, immune responses to cancer, heart disease, and neurodegenerative diseases [14]. Previous studies have suggested that p38 MAPK contributes to pathways promoting apoptosis and cancer progression [15]. Additionally, p38 has been implicated in an oncogenic role in NSCLC [16]. Importantly, phosphorylated p38 is markedly activated in lung cancer, and selective p38 inhibitors can suppress lung cancer progression [17, 18]. MKK3 and MKK6 are highly specific for p38 MAPKs [19]. Specific p38 isoforms are activated through MKK3/6-catalyzed phosphorylation of the conserved Thr-Gly-Tyr (TGY) motif in their activation loop [20]. The roles of MKK3 and MKK6 in p38α activation were illustrated in studies using fibroblasts isolated from Mkk3- and/or Mkk6-deficient mice, combined with siRNA techniques [21]. Specifically, MKK6 activates the p38γ isoform in response to TNFα, while MKK3 activates p38δ in response to ultraviolet radiation, hyperosmotic shock, anisomycin, or TNFα exposure [22]. MKK6 phosphorylates all four p38 MAPK family members, whereas MKK3 activates p38α, p38γ, and p38δ, but not p38β [19]. A key limitation in distinguishing MKK6 from MKK3 is the absence of a crystal structure for MKK3. Recently, a molecular model of the dynamic MKK6-p38α complex structure revealed two major contact points (αC-helix and αG-helix of MKK6) [23]. The selective activation of p38 MAPKs by MKK3 and MKK6 might contribute to the specificity of p38 MAPK signal transduction [21]. Moreover, p38α deletion upregulates MKK6 expression, while leaving MKK3 and MKK4 unaffected [24]. Despite efforts to develop selective MAPK inhibitors, no selective inhibitor for MKK6 over MKK3 has been identified.

Here, we describ sinensetin as a selective inhibitor of MKK6, but not MKK3, with anticancer activity against NSCLC cell lines and patient-derived xenograft-derived organoids (LPDXO) in an MKK6-dependent manner.

Materials and methods

Cell lines

Cell lines were purchased from the Cell Bank of the Chinese Academy of Sciences (Shanghai, China). Human NSCLC cell lines A549 (G12S KRAS, WT EGFR, WT TP53, WT PIK2CA, mutant KEAP1), H1299 (WT KRAS, Q61K NRAS, WT EGFR, R273H TP53, null KEAP1), and H460 (G12C KRAS, WT EGFR, 4AA deletion mutant TP53, E545K PIK3CA, mutant KEAP1) were cultured with RPMI-1640 medium, 10% fetal bovine serum (FBS; Biological Industries, Cromwell, CT, USA), and 1% antibiotic-antimycotic. NL20 lung cells were cultured in complete growth medium (Ham's F12 medium with 1.5 g/L sodium bicarbonate, 2.7 g/L glucose, 2.0 mM L-glutamine, 0.1 mM nonessential amino acids, 5 μg/ml insulin, 10 ng/ml epidermal growth factor, 1 μg/ml transferrin, 500 ng/ml hydrocortisone, and 4% FBS) at 37°C in a 5% CO_2 environment. Cells were cytogenetically tested and authenticated before freezing and each culture was maintained for a maximum of 8 weeks.

Reagents and antibodies

Sinensetin (purity: > 98% by HPLC) was purchased from ChemFaces (Wuhan, Hunan, China). Antibodies for detecting phosphorylated GSK3β (S9), ERK1/2 (T185/Y187), JNK (T183/T185), MKK3/6 (S189/S207), p38 (T180/Y182), AKT (S473), MKK6, and p21 were purchased from Cell Signaling Technology (Beverly, MA, USA). The GAPDH antibody was purchased from Proteintech (Wuhan, Hunan, China). Recombinant proteins such as MKK3, MKK6, and p38 for kinase assays were purchased from SignalChem (Richmond, BC, Canada).

MTT assay

A549, H1299 (1.5 × 10^3 cells per well), and H460 cells (0.8 × 10^3 cells per well) were seeded in 96-well plates and incubated for 24 h. Cells were treated with sinensetin for 72 h, followed by the addition of 20 μL MTT solution (Solarbio, Beijing, China) for 2 h at 37°C in a 5% CO_2 incubator. The cell culture medium was discarded and 150 μl of DMSO was added to dissolve formazan crystals via gentle agitation. Finally, cell growth was analyzed by measuring absorbance at 570 nm using a Thermo Multiskan plate reader (Thermo Fisher Scientific, Waltham, MA, USA).

Soft agar assay

A549 and H460 cells (8 × 10^3 cells per well), suspended in growth medium (RPMI 1640) supplemented with 10% FBS, were mixed with 0.3% agar with or without sinensetin at various concentrations and added as the top layer over a base layer of 0.6% agar with or without sinensetin at the same concentration under each experimental condition. Cultures were incubated at 37°C in a 5% CO_2 incubator for 2 weeks. Colonies were then imaged using an inverted microscope and quantified using Image-Pro Plus software (v.6) (Media Cybernetics, Rockville, MD, USA).

Focus forming assay

A549 and H1299 cells (8 × 10^2 cells per well) were suspended in a growth medium (RPMI 1640) supplemented with 10% FBS and subsequently seeded into 6-well plates. Then, cells were maintained at 37°C in a 5% CO_2 incubator for 1 week. Foci were subsequently stained with 0.4% crystal violet.

In vitro kinase assay

The kinase assay was performed following the instructions provided by Upstate Biotechnology (Billerica, MA, USA). Recombinant MKK3 or MKK6 (300 ng) protein was incubated with sinensetin at various concentrations at room temperature for 15 min. Then, p38 recombinant protein, ATP, and 1× buffer were added and incubated at 30°C for 30 min. The reaction was stopped by adding 10 μl of protein loading buffer, and samples were separated via SDS-PAGE. MKK3 or MKK6 activity was determined using an antibody specific to phosphorylated p38 (T180/Y182).

Cell cycle analysis

A549 and H1299 cells (2.5 × 10^4 or 4 × 10^4 cells per dish) were seeded in 60-mm culture dishes and incubated for 24 h. Cells were treated with sinensetin for 48 h in a growth medium with 10% FBS, harvested, and fixed in 1 ml of 70% cold ethanol. After rehydration, cells were digested with RNase (100 μg/ml) and stained with propidium iodide (20 μg/ml). Finally, cells were analyzed via flow cytometry.

Establish MKK6 knockout cell lines

A549 and H1299 MKK6 knockout (KO) cell lines were generated using the CRISPR/Cas9 system. gRNA sequences targeting MKK6 exon were designed (sg#3: forward: caccgataggcaagaagcgaaaccc, reverse: aaacgggtttcgcttcttgcctatc; sg#4: forward: caccgttcaccctacatgaatccaa, reverse: aaacttggattcatgtagggtgaac). The Lenti-CRISPR-V2 vector was linearized with ESP3I and ligated with gRNAs using T4 DNA ligase. Lentiviral particles containing the CRISPR/Cas9 and gRNA constructs were used to transduce cells. Puromycin (5 μg/mL) selection was applied 48 h post-infection. Monoclonal cell lines were established via limiting dilution. KO clones were screened through Western blotting and confirmed via DNA sequencing of the targeted genomic region.

Surface plasmon resonance

The surface plasmon resonance (SPR) assay was performed according to the instructions provided with the Biacore T200 (GE Healthcare, England, UK) instrument. MKK6 protein was immobilized onto a CM5 sensor chip. Next, the chip was equilibrated with PBS. A concentration series of sinensetin, dissolved in 5% DMSO in PBS, was perfused over the CM5 chip at a flow rate of 30 μL/min to assess the binding affinity between sinensetin and MKK6. The T200 evaluation state model was utilized to analyze binding affinity data and representative data were re-plotted.

Western blotting

Proteins were quantified using a BCA kit (Solarbio) following the manufacturer's proto-

col. Proteins were separated by SDS-PAGE and transferred to polyvinylidene difluoride membranes (Amersham Biosciences, Piscataway, NJ, USA). Membranes were blocked with 5% nonfat dry milk (Solarbio) in TBST (TBS with 1% Tween 20) for 1 h at room temperature. After blocking, the membranes were washed three times with TBST and incubated overnight at 4°C with primary antibodies. The next day, the membranes were washed three times with TBST and then incubated with a horseradish peroxidase-linked secondary antibody for 1 h. Finally, the membranes were washed three times with TBST, and the immunoreactive proteins were detected using the Thermo Scientific SuperSignal West Pico PLUS Chemiluminescent Substrate (Thermo Fisher Scientific) and the ImageQuant LAS4000 system (GE Healthcare, Piscataway, NJ, USA).

In silico molecular docking analysis of sinensetin with MKK6 and MKK3

To study the molecular docking of sinensetin with MKK6 and MKK3, *in silico* analysis was performed using the DiffDock-L web server. The MKK6 crystal structure (5eti.pdb) was obtained from the PDB Bank and the predicted crystal structure of MKK3 was obtained from AlphaFold (http://alphafold.ebi.ac.uk) [25, 26]. Information regarding these structures was downloaded and analyzed. The results of the top five docking models for sinensetin with MKK6 or MKK3 are presented.

Patient-derived lung tumor xenografts (PDX)

Severe combined immunodeficiency (SCID) female mice (6-9 weeks old) (Cyagen Biosciences Lnc., Suzhou, China) were maintained under "specific pathogen-free" conditions based on the guidelines established by the Zhengzhou University Institutional Animal Care and Use Committee (SYXK 2021-0011, 2021-07-03~ 2026-07-29). Human lung tumor specimens were obtained from the Affiliated Cancer Hospital in Zhengzhou University. The anonymized clinical information of the participant is provided in Supplementary Table 1. LG70 NSCLC patient tissues were cut into small pieces and inoculated into the back of the neck of each mouse (n = 3). Mice were monitored until tumors reached approximately 1.5 cm^3 total volume, at which time the mice were euthanized, and the tumor tissues were extracted.

Organoid culture and analysis

LPDXOs were generated from lung patient-derived xenograft models according to protocols outlined by Shi et al. [36]. The dissociation procedure involved transferring and mincing LG70 PDX tumor tissue, followed by incubation with HBSS-DF, collagenase IV (Thermo, 1710-4019), and Y-27632 (MCE, HY-10071) additives to enhance single-cell yields. Subsequently, tissue fragments were filtered, and the collected cell suspension was centrifuged and resuspended. For LPDXO initiation, cells were seeded after the thawing of matrigel and pre-warming of the plate and organoid medium. Organoid generation was performed in a 96-well plate, where cells were transferred, centrifuged, and resuspended in matrigel before being dispensed into the wells. After solidification, the organoid medium containing different doses of sinensetin was added, and organoids were cultivated for 16 d. Photographs of the organoids were taken during organoid cultivation. On day 16, MTT solution was added, photographs were captured, and the optical density was measured at 570 nm using a Thermo Multiskan plate reader.

Statistical analysis

All quantitative results are expressed as mean values ± standard deviation (SD) or ± standard error (SE). Significant differences ($P < 0.05$) were compared using the Student's t-test or one-way analysis of variance (ANOVA).

Results

Sinensetin inhibits anchorage-dependent and -independent NSCLC cell growth

Sinensetin, a flavonoid compound (**Figure 1A**) derived from *Orthosiphon* species, is employed in traditional medicine [8]. To determine the potential cytotoxic effects of sinensetin, human normal NL20 lung cells were treated with increasing concentrations of sinensetin. Sinensetin had little or no cytotoxic effects on healthy lung cells. Only limited cytotoxicity on NL20 cells was observed at 100 μM (**Figure 1B**). The effect of sinensetin on NSCLC cell growth was investigated. Cells were treated with different doses and incubated for 72 h, and the viable cells were analyzed via the MTT assay. Sinensetin significantly suppressed the

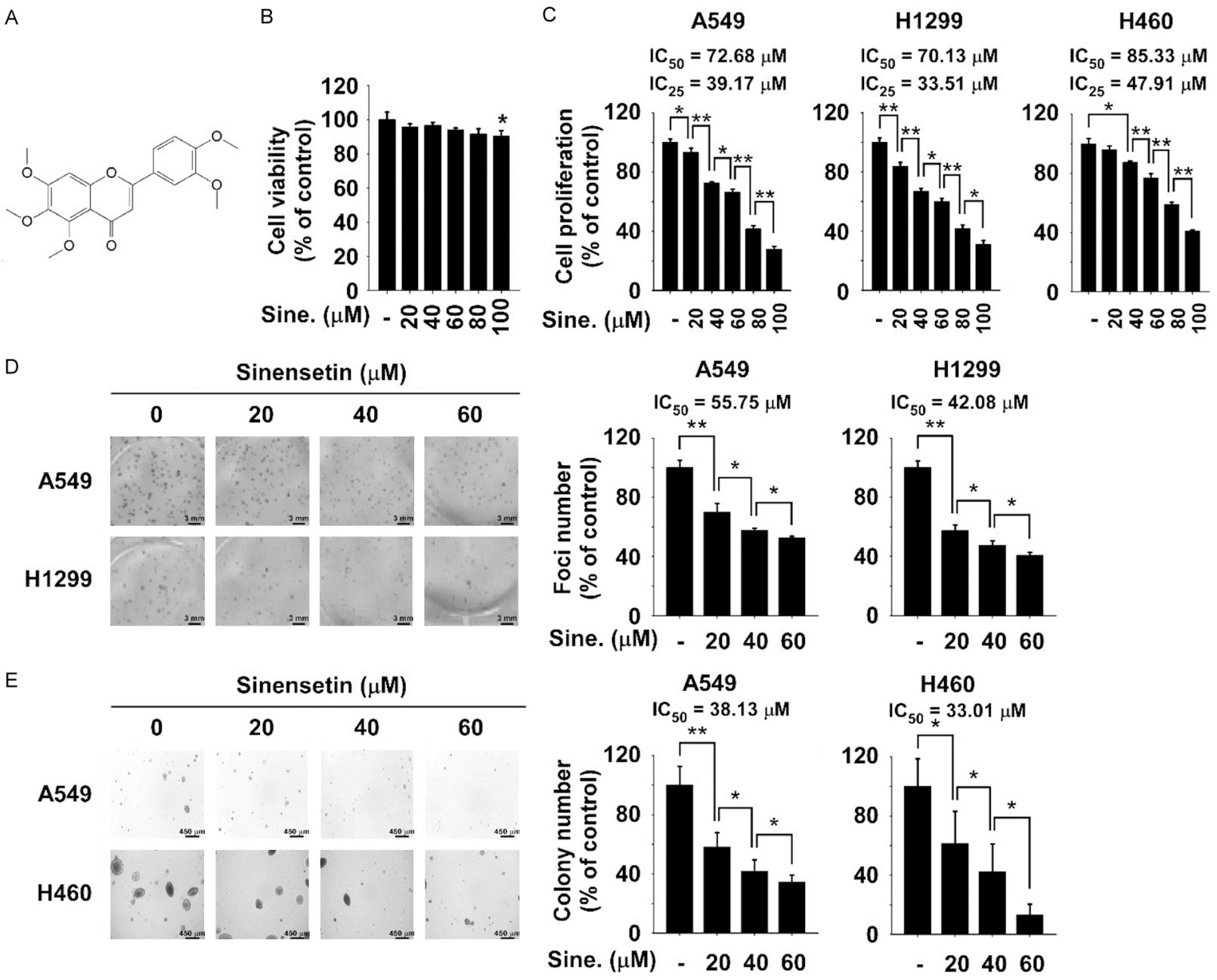
A
B
Cell viability (% of control)
Sine. (μM) - 20 40 60 80 100
C
A549
IC50 = 72.68 μM
IC25 = 39.17 μM
H1299
IC50 = 70.13 μM
IC25 = 33.51 μM
H460
IC50 = 85.33 μM
IC25 = 47.91 μM
Cell proliferation (% of control)
D
Sinensetin (μM)
0 20 40 60
A549
H1299
A549
IC50 = 55.75 μM
H1299
IC50 = 42.08 μM
Foci number (% of control)
E
Sinensetin (μM)
0 20 40 60
A549
H460
A549
IC50 = 38.13 μM
H460
IC50 = 33.01 μM
Colony number (% of control)

Figure 1. Sinensetin inhibits growth of NSCLC cells. (A) Chemical structure of sinensetin. (B) Effects of sinensetin on the viability of human normal NL20 lung cells, analyzed using the MTT assay. (C) Effects of sinensetin on NSCLC cell growth were also assessed using the MTT assay. (D) Effects of sinensetin on focus formation, evaluated using the focus formation assay. (E) Effects of sinensetin on anchorage-independent NSCLC cell growth, with colonies counted using microscopy and Image-Pro PLUS (v.6) software. For (B-E), data represent means ± SD values from three independent experiments, each with triplicate samples, analyzed using one-way ANOVA with Tukey's honestly significant difference (HSD) post hoc test. Asterisks (*, **) indicate significant ($P < 0.05$, $P < 0.01$) differences.

anchorage-dependent growth of NSCLC cells in a dose-dependent manner (**Figure 1C**). Next, we investigated the effect of sinensetin on foci formation (**Figure 1D**) and anchorage-independent growth (**Figure 1E**) in NSCLC cells. Treatment with sinensetin strongly inhibited both foci and anchorage-independent growth compared to untreated controls in a dose-dependent manner (**Figure 1D**, **1E**).

Sinensetin increases G1-phase cell cycle arrest in NSCLC cells

Flow cytometry analysis was performed to determine the effect of 48-hour sinensetin treatment on cell cycle progression. Sinensetin weakly but significantly induced G1-phase cell cycle arrest in NSCLC cells (**Figure 2A**, **2B**). Furthermore, the effect of sinensetin on the expression levels of p21, a mediator of G1-phase cell cycle arrest, was assessed. Treatment with sinensetin for 48 h strongly induced p21 expression in NSCLC cells (**Figure 2C**).

Sinensetin inhibits LPDXO growth

LPDXOs expressed relatively high levels of MKK6 compared to normal NL20 cells (Supplementary Figure 1). LPDXOs were treated with varying concentrations of sinensetin and incubated for 16 d to investigate its effect on the growth of NSCLC patient-derived xenograft organoids. LPDXO growth was significantly suppressed with sinensetin treatment (**Figure 3A**). Similarly, the MTT assay confirmed that sinensetin reduced LPDXO growth (**Figure 3B**). LPDXOs treated with sinensetin exhibited strong growth inhibition compared to untreated controls (**Figure 3C**).

Sinensetin is a novel MKK6 inhibitor

To identify potential molecular targets of sinensetin, we assessed its effects on various signaling molecules in NSCLC cells following a 12-hour treatment of A549 and H1299 cells with sinensetin. Sinensetin substantially reduced the levels of phospho (p)-p38 in both NSCLC cell lines, while the levels of other phosphorylated proteins remained unchanged (**Figure 4A**). Additionally, p-AKT levels were reduced in H1299 cells but not in A549 cells, indicating that sinensetin could inhibit the kinase activities of MKK3 and/or MKK6. To test this hypothesis, *in vitro* kinase assays were performed using recombinant active MKK6 or MKK3 with an inactive (unphosphorylated) p38 protein as a substrate of MKK3/6. Notably, sinensetin reduced MKK6-mediated p38α phosphorylation in a dose-dependent manner (**Figure 4B**), while it did not affect MKK3-mediated p38α phosphorylation (**Figure 4C**). Furthermore, SPR analysis confirmed the direct binding of sinensetin with MKK6, revealing an affinity of 66.27 μM (**Figure 4D**). To gain deeper insight into the differential inhibition of MKK6 activity by sinensetin, we performed in silico molecular docking analyses with MKK3 or MKK6. The top five docking models were selected based on molecular docking scores. The findings indicated that sinensetin was docked at the αC-helix and αG-helix of MKK6 (**Figure 4E**, *upper panel*), whereas it interacted only with the αC-helix of MKK3 (**Figure 4E**, *lower panel*). These results suggest that sinensetin specifically binds to the αG-helix of MKK6, thereby inhibiting its catalytic activity. Since αG-helix residues are crucial in interactions with p38α, and mutations in this region result in reduced p38α signaling [23], the selective binding of sinensetin to the αG-helix may inhibit the MKK6-p38α interaction without affecting MKK3-p38α signaling. Further validation is necessary to elucidate the mechanism of selectivity of sinensetin for MKK6 over MKK3. Overall, these results suggest that sinensetin functions as a selective inhibitor of MKK6.

MKK6 knockout suppresses NSCLC cell growth

To examine the clinical relevance of MKK6 in lung cancer, RNA-seq data from the Cancer Genome Atlas Program (TCGA) was used to analyze MKK6 mRNA expression levels in

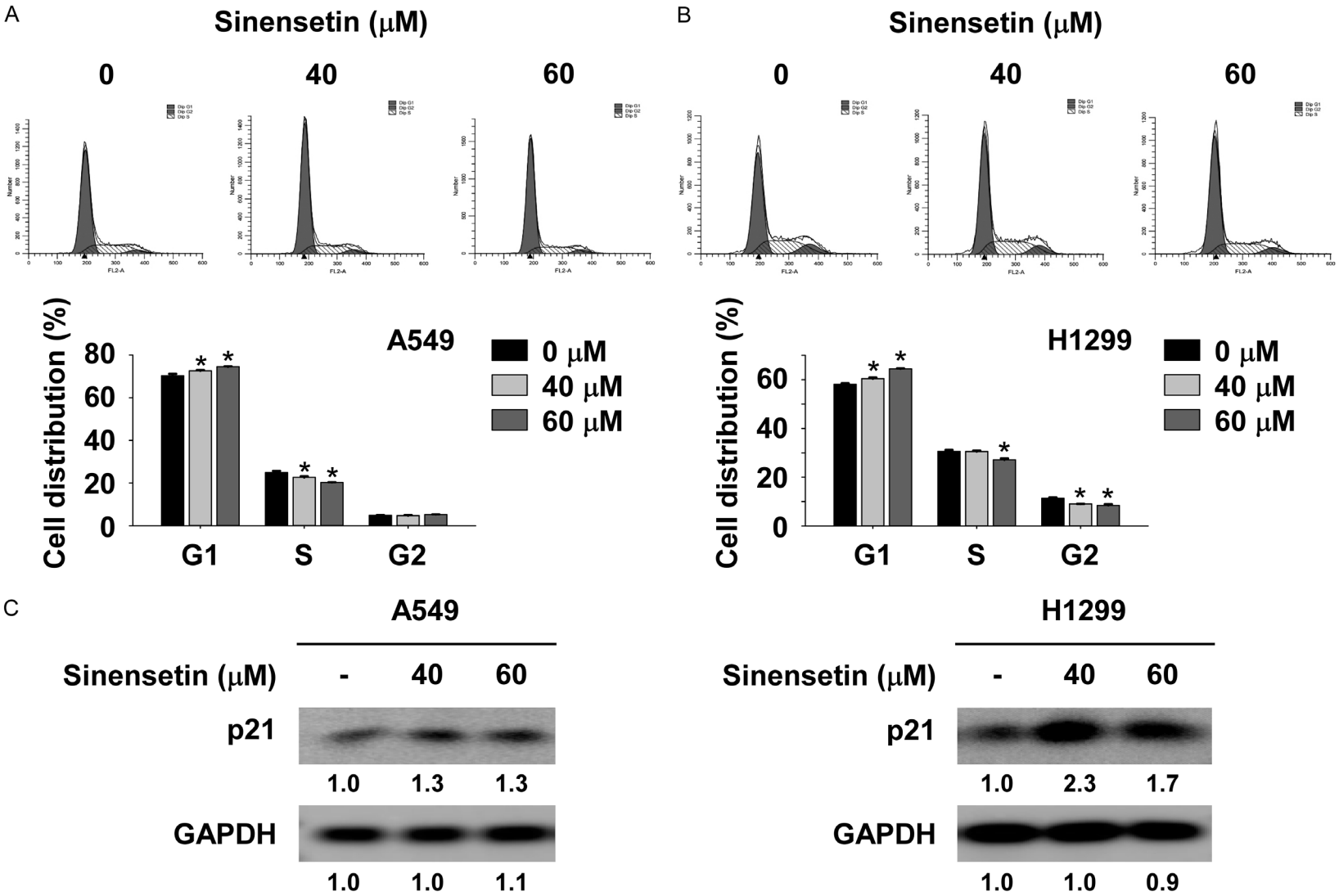

Figure 2. Sinensetin induces G1-phase cell cycle arrest. A, B. Effects of sinensetin on the cell cycle distribution of A549 and H1299 NSCLC cells, as examined by fluorescence-activated cell sorting (FACS). Data are indicated as means ± SD values from three independent experiments, with one-way ANOVA and Dunnett's post hoc test used for statistical analysis. The asterisk (*) indicates a significant ($P < 0.05$) differences. C. Effects of sinensetin on p21 protein expression levels, examined via Western blotting. Similar results were observed from three independent experiments and band density was measured using the Image J (NIH) software program.

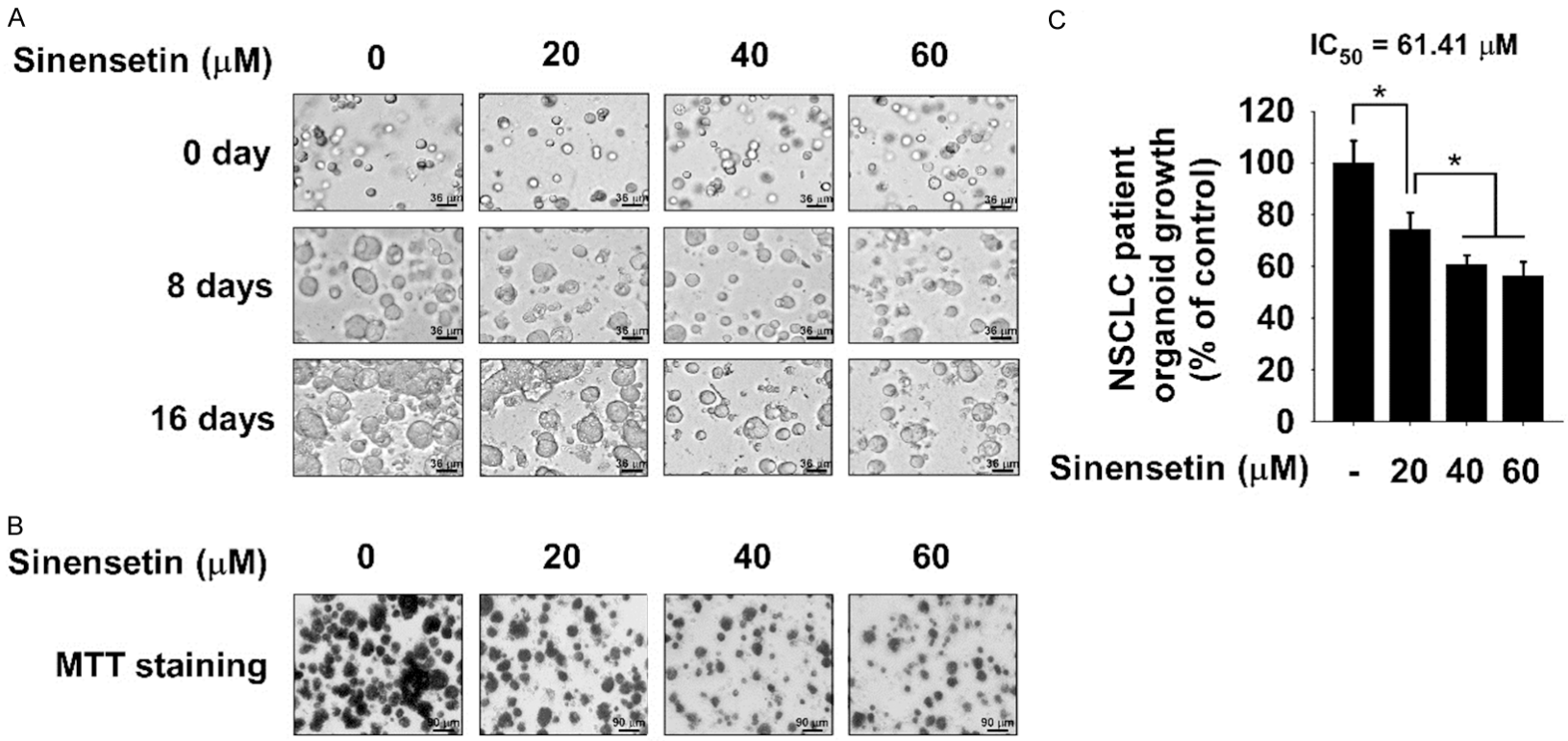

Figure 3. Sinensetin suppresses LPDXO growth. (A, B) Representative images after sinensetin treatment (A) are shown. Relative growth of LPDXOs, measured using the MTT assay (B). (C) Effect of sinensetin on the growth of LPDXOs. LPDXO growth was analyzed using the MTT assay, with data shown as means ± SD values derived from three independent experiments. Asterisks (*, **) indicate significant ($P < 0.05$, $P < 0.01$) differences.

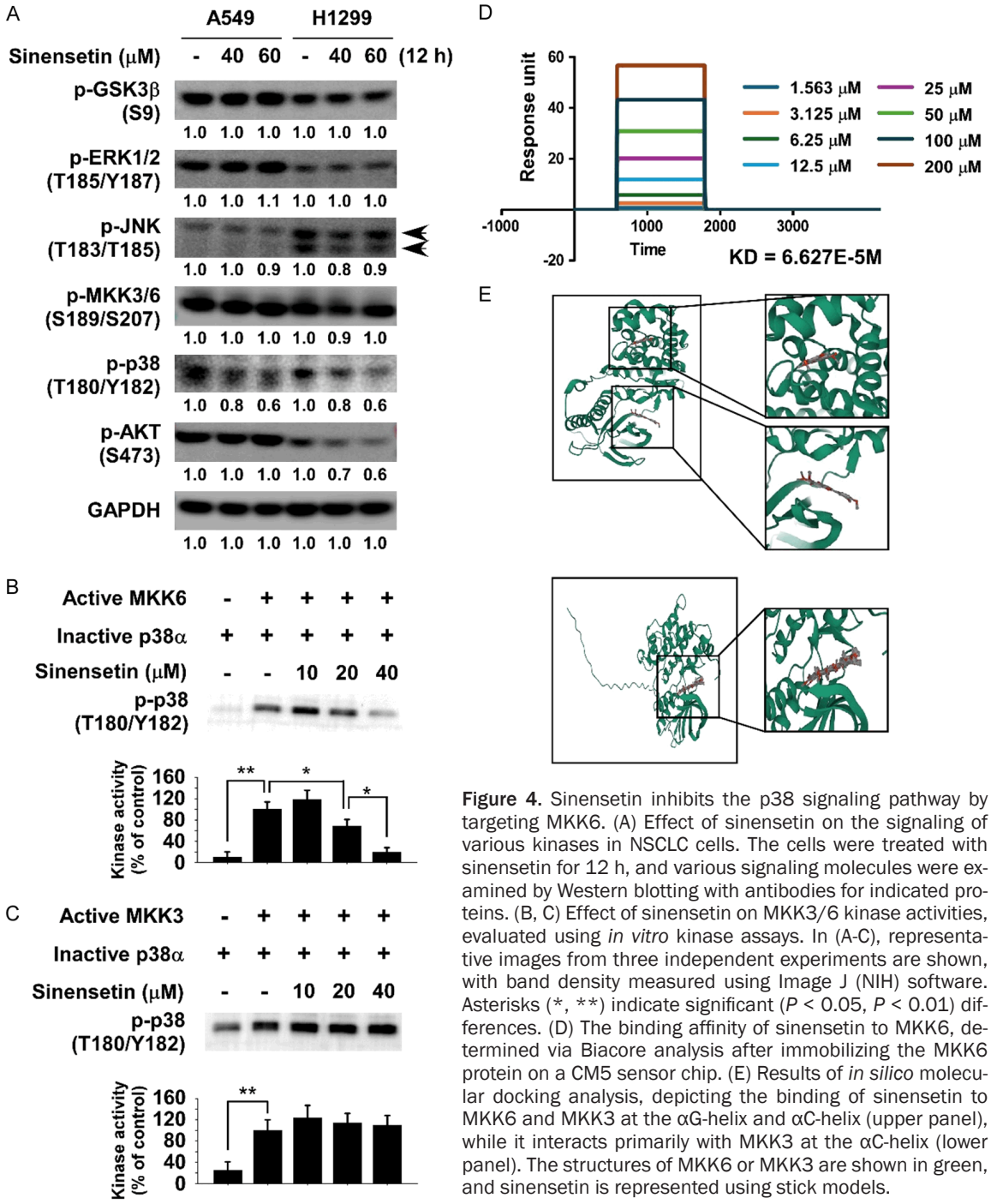

Figure 4. Sinensetin inhibits the p38 signaling pathway by targeting MKK6. (A) Effect of sinensetin on the signaling of various kinases in NSCLC cells. The cells were treated with sinensetin for 12 h, and various signaling molecules were examined by Western blotting with antibodies for indicated proteins. (B, C) Effect of sinensetin on MKK3/6 kinase activities, evaluated using *in vitro* kinase assays. In (A-C), representative images from three independent experiments are shown, with band density measured using Image J (NIH) software. Asterisks (*, **) indicate significant ($P < 0.05$, $P < 0.01$) differences. (D) The binding affinity of sinensetin to MKK6, determined via Biacore analysis after immobilizing the MKK6 protein on a CM5 sensor chip. (E) Results of *in silico* molecular docking analysis, depicting the binding of sinensetin to MKK6 and MKK3 at the αG-helix and αC-helix (upper panel), while it interacts primarily with MKK3 at the αC-helix (lower panel). The structures of MKK6 or MKK3 are shown in green, and sinensetin is represented using stick models.

NSCLC and normal lung tissues. MKK6 mRNA levels were significantly increased in NSCLC tissues compared to normal lung tissues (**Figure 5A**). Furthermore, Kaplan-Meier analysis (http://kmplot.com/analysis) showed that NSCLC patients with elevated MKK6 expression levels exhibited poorer overall survival than patients with low MKK6 expression levels (**Figure 5B**). To determine the effect of MKK6 depletion on NSCLC growth, we established MKK6 knockout cells (sgMKK6 #3 and #4) and validated MKK6 depletion in comparison to the control (sgC) via Western blotting (**Figure 5C**). MKK6 depletion inhibited NSCLC cell growth (**Figure 5D**) and foci formation (**Figure 5E**).

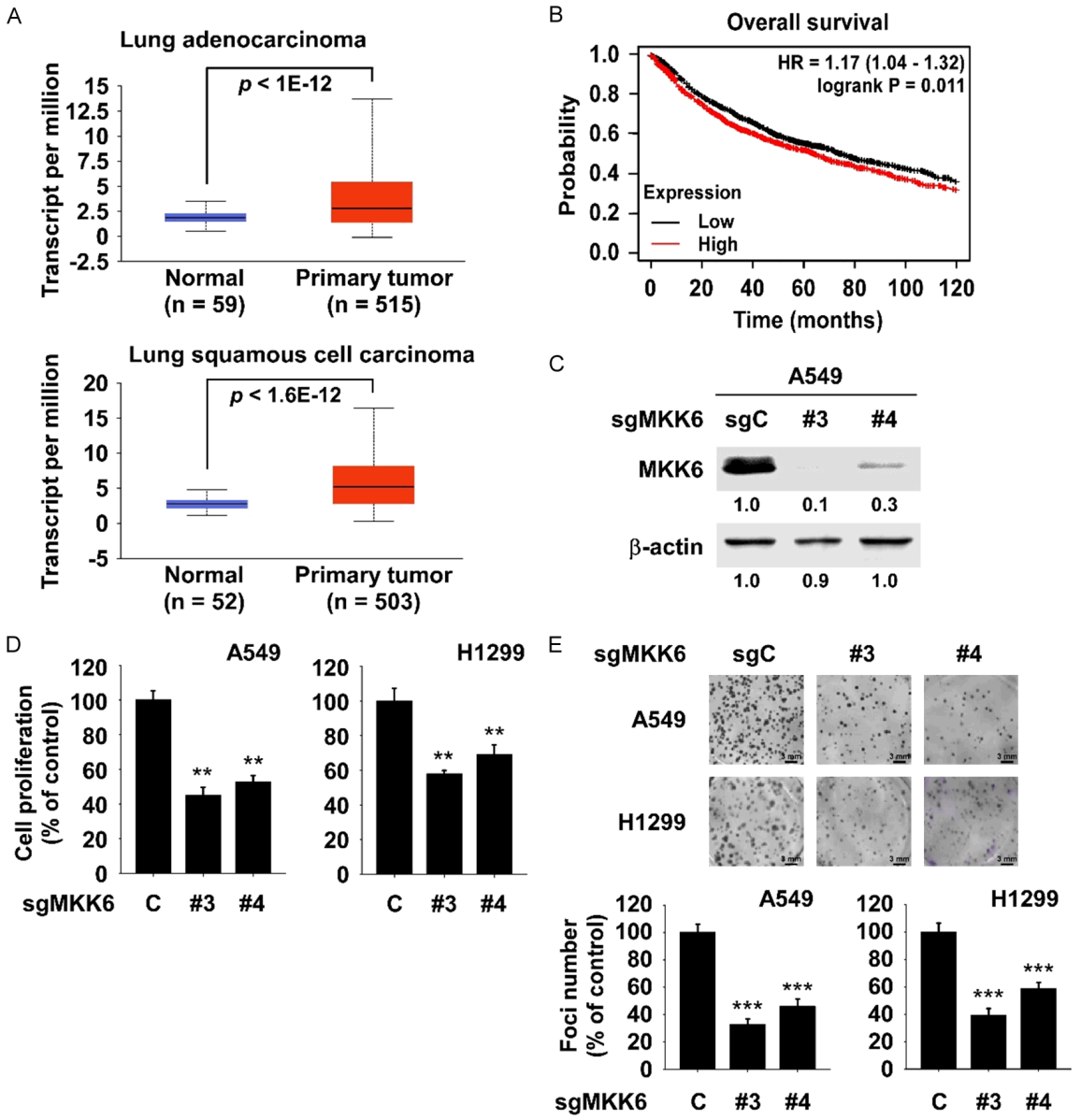

Figure 5. Role of MKK6 as a therapeutic target in NSCLC cells. (A) MKK6 expression levels in lung adenocarcinoma and lung squamous cell carcinoma cells, based on data obtained from the TCGA database. (B) Prognostic significance of MKK6 expression in lung cancer, analyzed using the Kaplan-Meier plotter. (C) Efficacy of MKK6 knockdown, determined using Western blotting. (D) Effect of MKK6 knockdown on NSCLC cell growth, determined using the MTT assay. (E) Effect of MKK6 knockdown on focus formation in NSCLC cells. Cells were incubated for 1 week, and the number of foci was counted. For (D and E), data are shown as means ± SD values derived from three independent experiments. Asterisks (**, ***) indicate significant ($P < 0.01$, $P < 0.001$) differences.

Inhibitory effects of sinensetin are dependent on MKK6 expression levels

To validate the dependency of MKK6 on the effects of sinensetin, sgC or sgMKK6 cells were treated with sinensetin and NSCLC cell growth was evaluated using MTT or foci formation assays. sgMKK6 cells were more resistant to the inhibitory effect of sinensetin on cell growth and foci formation compared to sgControl cells (**Figure 6A**, **6B**).

Discussion

Small molecule natural products have been a major source of medicine for several years. For

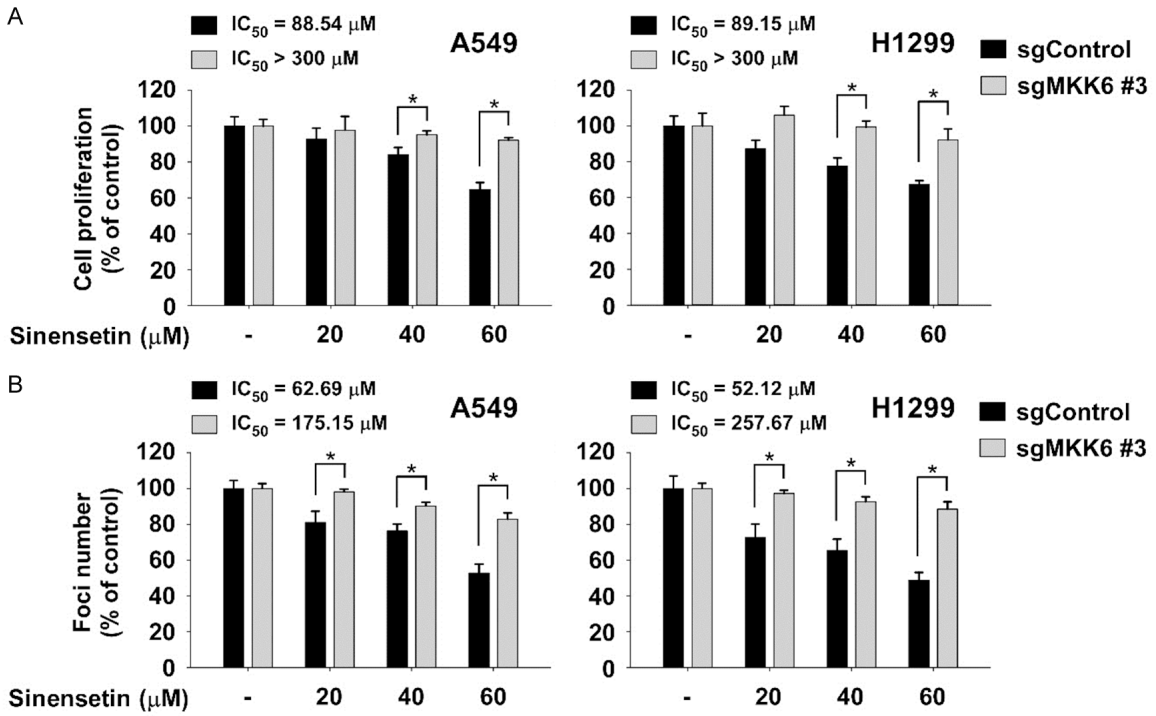

Figure 6. MKK6-dependent anticancer activity of sinensetin. (A, B) MKK6-dependent inhibitory effect of sinensetin on NSCLC cell growth (A) and foci formation ability (B). Treatment of sgMKK6 or sgControl cells with or without sinensetin, respectively. Data for both panels are shown as means ± SD values derived from three independent experiments. Asterisks (*) indicate significant ($P < 0.05$) differences.

example, aspirin (acetylsalicylic acid) precursors have been used as medicine for millennia [27]. However, the primary target for acetylsalicylic acid was not identified until the 1970s [28], and research on aspirin target ID has been continued [29]. Target ID is a key step toward developing new drug entities in modern medicine, enabling the structure-action relationship (SAR)-based modification of chemicals that accelerate the optimization of their pharmacological activities. Despite advances in technology, target ID remains a significant barrier to developing drugs using natural compounds.

Sinensetin, a plant-derived polymethoxylated flavonoid, exhibits various biological activities, though its molecular targets and potential therapeutic effects in NSCLC remain unexplored. Here, we demonstrate that sinensetin inhibits NSCLC growth by directly targeting MKK6. Our signaling pathway analyses and *in vitro* kinase assay results revealed that sinensetin significantly suppressed MKK6-p38α signaling pathway and selectively inhibited MKK6 kinase activity without affecting MKK3 activity (**Figure 4A-C**). SPR analysis further confirmed the binding of sinensetin to MKK6 with an affinity of 66.27 μM (**Figure 4D**). Importantly, we investigated how sinensetin affects only MKK6 activity. Our top five *in silico* molecular docking analyses showed that sinensetin was effectively docked at the αG-helix of MKK6, but not MKK3 (**Figure 4E**). However, these findings could not elucidate the molecular basis of differential interactions between sinensetin and the αC-helix of MKK6 and MKK3. Further studies are needed to explore the binding dynamics between sinensetin and αC and αG-helix of MKKs. Since the αG-helix motif is indispensable for the binding of MKK6 to p38α [23], our results suggest that the binding of sinensetin to the αG-helix of MKK6 may inhibit MKK6-p38α interactions. MKK3 and MKK6 are essential for classical p38 activation via the phosphorylation of threonine (T180) and tyrosine (Y182) residues within the active loop of p38 [30]. Both MKK3 and MKK6 are essential for activating p38γ and p38β in response to different cellular stresses, and for p38δ activation during hyperosmotic stress. However, MKK6 plays a

primary role in activating p38γ in response to TNFα and anisomycin treatment [22]. Until now, there are no known inhibitors that selectively target MKK6 and MKK3. Developing isoform-selective inhibitors is critical for both basic research and new drug development. Although the molecular mechanism underlying the selective targeting of MKK6 over MKK3 by sinensetin needs to be elucidated in future studies, our findings suggest that sinensetin could serve as a specific MKK6 inhibitor. This selectivity offers potential for therapeutic strategies in NSCLC when combined with other treatment modalities.

Compelling evidence supports the dual role of p38 in cancer, acting as both a tumor suppressor (by regulating proliferation, differentiation, and apoptosis) and a tumor promoter (by inducing cell survival, proliferation, and angiogenesis) in a cellular context-dependent manner [31]. In NSCLC, p38 isoforms were significantly upregulated, with only p38α expression significantly associated with tumor stages [32]. In addition, elevated p38α expression levels were correlated with higher malignancy and poorer prognosis in lung adenocarcinoma patients, further promoting $Kras^{G12V}$-driven lung tumor progression [33]. While the oncogenic role of the p38α signaling pathway in NSCLC is well established, the clinical implications of MKK6 in NSCLC have not been fully investigated due to the lack of specific inhibitors for MKK6. Here, we first discovered sinensetin the first selective inhibitor of MKK6, and identified the negative correlation between high MKK6 expression levels and low survival rates in lung cancer patients (**Figure 5A** and **5B**).

The finding that sinensetin induces cell cycle arrest in NSCLC cells through MKK6 inhibition is unsurprising. Specifically, p38 modulates the phosphorylation of several proteins in the CDK-RB-E2F axis, thereby affecting G1 arrest [34]. The MAPK pathway promotes oncogenic MYC protein stability to enhance inhibitory effects by modulating p21 expression [35]. Our results showed that sinensetin upregulates p21 expression, which increases levels of G1-phase cell cycle arrest in lung cancer cells (**Figure 2C**). Overall, we suggest that sinensetin induces G1-phase cell cycle arrest by directly targeting MKK6 activity to reduce p38 activation in NSCLC cells.

In conclusion, this study establishes sinensetin as a selective MKK6 inhibitor that suppresses NSCLC growth and induces G1-phase cell cycle arrest. Further investigation into its inhibition of MKK6-p38 pathways could reveal novel strategies for targeted therapy and chemoprevention in NSCLC.

Acknowledgements

This work was supported by the National Natural Science Foundation of China (NSFC) under grant number (82103193), and by the Bio & Medical Technology Development Program of the National Research Foundation of Korea (NRF), funded by the Ministry of Science & ICT, with the following grant numbers: RS-2022-NR74902 for Y.W.Y.; RS-2022-NR072821 for Y.S.S.; and RS-2023-00237259 for D.J.K.

Disclosure of conflict of interest

None.

Abbreviations

MKK3/6, mitogen-activated protein kinase kinase 3/6; GSK3β, glycogen synthase kinase 3 beta; ERK, extracellular signal-regulated kinase; JNK, c-Jun N-terminal kinase; p38, mitogen-activated protein kinase 14; AKT, protein kinase B; LPDXOs, lung patient-derived xenograft organoids.

Address correspondence to: Dr. Yong Weon Yi, Department of Biochemistry, College of Medicine, Dankook University, No. 119 Dandae-ro, Dongnam-gu, Cheonan-si 31116, Chungcheongnam-do, Republic of Korea. Tel: +82-41-550-3974; Fax: +82-41-559-7940; E-mail: yongweon_yi@dankook.ac.kr; Dr. Dong Joon Kim, China-US (Henan) Hormel Cancer Institute, No. 127 Dongming Road, Zhengzhou 450008, Henan, China. Tel: +86-371-6558-7909; Fax: +86-371-6558-7227; E-mail: djkim@hci-cn.org; Department of Microbiology, College of Medicine, Dankook University, No. 119 Dandae-ro, Dongnam-gu, Cheonan-si 31116, Chungcheongnam-do, Republic of Korea. Tel: +82-41-550-3873; Fax: +82-41-559-7940; E-mail: djkim407@dankook.ac.kr

References

[1] Atanasov AG, Zotchev SB, Dirsch VM, Orhan IE, Banach M, Rollinger JM, Barreca D, Weckwerth W, Bauer R, Bayer EA, Majeed M, Bishay-

ee A, Bochkov V, Bonn GK, Braidy N, Bucar F, Cifuentes A, D'Onofrio G, Bodkin M, Diederich M, Dinkova-Kostova AT, Efferth T, Bairi KE, Arkells N, Fan TP, Fiebich BL, Freissmuth M, Georgiev MI, Gibbons S, Godfrey KM, Gruber CW, Heer J, Huber LA, Ibanez E, Kijjoa A, Kiss AK, Lu A, Macias FA, Miller MJS, Mocan A, Müller R, Nicoletti F, Perry G, Pittalà V, Rastrelli L, Ristow M, Russo GL, Silva AS, Schuster D, Sheridan H, Skalicka-Woźniak K, Skaltsounis L, Sobarzo-Sánchez E, Bredt DS, Stuppner H, Sureda A, Tzvetkov NT, Vacca RA, Aggarwal BB, Battino M, Giampieri F, Wink M, Wolfender JL, Xiao J, Yeung AWK, Lizard G, Popp MA, Heinrich M, Berindan-Neagoe I, Stadler M, Daglia M, Verpoorte R and Supuran CT. Natural products in drug discovery: advances and opportunities. Nat Rev Drug Discov 2021; 20: 200-216.

[2] Li G, Peng X, Guo Y, Gong S, Cao S and Qiu F. Currently available strategies for target identification of bioactive natural products. Front Chem 2021; 9: 761609.

[3] Luo Y, Xu D, Cao Z, Chen Q, Wang L, Fang G and Pang Y. Traditional therapies of Zhuang medicine improve pain and joint dysfunction of patients in rheumatoid arthritis. Medicine (Baltimore) 2020; 99: e22264.

[4] Beaux D, Fleurentin J and Mortier F. Effect of extracts of Orthosiphon stamineus benth, Hieracium pilosella L., Sambucus nigra L. and Arctostaphylos uva-ursi (L.) spreng. in rats. Phytother Res 1999; 13: 222-225.

[5] Adam Y, Somchit MN, Sulaiman MR, Nasaruddin AA, Zuraini A, Bustamam AA and Zakaria ZA. Diuretic properties of Orthosiphon stamineus Benth. J Ethnopharmacol 2009; 124: 154-158.

[6] Mohamed EA, Siddiqui MJ, Ang LF, Sadikun A, Chan SH, Tan SC, Asmawi MZ and Yam MF. Potent α-glucosidase and α-amylase inhibitory activities of standardized 50% ethanolic extracts and sinensetin from Orthosiphon stamineus Benth as anti-diabetic mechanism. BMC Complement Altern Med 2012; 12: 176.

[7] Manshor NM, Dewa A, Asmawi MZ, Ismail Z, Razali N and Hassan Z. Vascular reactivity concerning orthosiphon stamineus benth-mediated antihypertensive in aortic rings of spontaneously hypertensive rats. Int J Vasc Med 2013; 2013: 456852.

[8] Liu S, Qin HH, Ji XR, Gan JW, Sun MJ, Tao J, Tao ZQ, Zhao GN and Ma BX. Virtual screening of Nrf2 dietary-derived agonists and safety by a new deep-learning model and verified in vitro and in vivo. J Agric Food Chem 2023; 71: 8038-8049.

[9] Han Jie L, Jantan I, Yusoff SD, Jalil J and Husain K. Sinensetin: an insight on its pharmacological activities, mechanisms of action and toxicity. Front Pharmacol 2021; 11: 553404.

[10] Liu Z, Liu R, Wang R, Dai J, Chen H, Wang J and Li X. Sinensetin attenuates IL-1β-induced cartilage damage and ameliorates osteoarthritis by regulating SERPINA3. Food Funct 2022; 13: 9973-9987.

[11] Kim SM, Ha SE, Lee HJ, Rampogu S, Vetrivel P, Kim HH, Venkatarame Gowda Saralamma V, Lee KW and Kim GS. Sinensetin induces autophagic cell death through p53-Related AMPK/mTOR signaling in hepatocellular carcinoma HepG2 cells. Nutrients 2020; 12: 2462.

[12] Li X, Li Y, Wang Y, Liu F, Liu Y, Liang J, Zhan R, Wu Y, Ren H, Zhang X and Liu J. Sinensetin suppresses angiogenesis in liver cancer by targeting the VEGF/VEGFR2/AKT signaling pathway. Exp Ther Med 2022; 23: 360.

[13] Cargnello M and Roux PP. Activation and function of the MAPKs and their substrates, the MAPK-activated protein kinases. Microbiol Mol Biol Rev 2011; 75: 50-83.

[14] Cuadrado A and Nebreda AR. Mechanisms and functions of p38 MAPK signalling. Biochem J 2010; 429: 403-417.

[15] Stramucci L, Pranteda A and Bossi G. Insights of crosstalk between p53 protein and the MKK3/MKK6/p38 MAPK signaling pathway in cancer. Cancers (Basel) 2018; 10: 131.

[16] Deng K, Liu L, Tan X, Zhang Z, Li J, Ou Y, Wang X, Yang S, Xiang R and Sun P. WIP1 promotes cancer stem cell properties by inhibiting p38 MAPK in NSCLC. Signal Transduct Target Ther 2020; 5: 36.

[17] Campbell RM, Anderson BD, Brooks NA, Brooks HB, Chan EM, De Dios A, Gilmour R, Graff JR, Jambrina E, Mader M, McCann D, Na S, Parsons SH, Pratt SE, Shih C, Stancato LF, Starling JJ, Tate C, Velasco JA, Wang Y and Ye XS. Characterization of LY2228820 dimesylate, a potent and selective inhibitor of p38 MAPK with antitumor activity. Mol Cancer Ther 2014; 13: 364-374.

[18] Greenberg AK, Basu S, Hu J, Yie TA, Tchou-Wong KM, Rom WN and Lee TC. Selective p38 activation in human non-small cell lung cancer. Am J Respir Cell Mol Biol 2002; 26: 558-564.

[19] Ben-Levy R, Hooper S, Wilson R, Paterson HF and Marshall CJ. Nuclear export of the stress-activated protein kinase p38 mediated by its substrate MAPKAP kinase-2. Curr Biol 1998; 8: 1049-1057.

[20] Martínez-Limón A, Joaquin M, Caballero M, Posas F and de Nadal E. The p38 pathway: from biology to cancer therapy. Int J Mol Sci 2020; 21: 1913.

[21] Brancho D, Tanaka N, Jaeschke A, Ventura JJ, Kelkar N, Tanaka Y, Kyuuma M, Takeshita T, Flavell RA and Davis RJ. Mechanism of p38 MAP kinase activation in vivo. Genes Dev 2003; 17: 1969-1978.

[22] Remy G, Risco AM, Iñesta-Vaquera FA, González-Terán B, Sabio G, Davis RJ and Cuenda A. Differential activation of p38MAPK isoforms by MKK6 and MKK3. Cell Signal 2010; 22: 660-667.
[23] Juyoux P, Galdadas I, Gobbo D, von Velsen J, Pelosse M, Tully M, Vadas O, Gervasio FL, Pellegrini E and Bowler MW. Architecture of the MKK6-p38α complex defines the basis of MAPK specificity and activation. Science 2023; 381: 1217-1225.
[24] Ambrosino C, Mace G, Galban S, Fritsch C, Vintersten K, Black E, Gorospe M and Nebreda AR. Negative feedback regulation of MKK6 mRNA stability by p38alpha mitogen-activated protein kinase. Mol Cell Biol 2003; 23: 370-381.
[25] Jumper J, Evans R, Pritzel A, Green T, Figurnov M, Ronneberger O, Tunyasuvunakool K, Bates R, Žídek A, Potapenko A, Bridgland A, Meyer C, Kohl SAA, Ballard AJ, Cowie A, Romera-Paredes B, Nikolov S, Jain R, Adler J, Back T, Petersen S, Reiman D, Clancy E, Zielinski M, Steinegger M, Pacholska M, Berghammer T, Bodenstein S, Silver D, Vinyals O, Senior AW, Kavukcuoglu K, Kohli P and Hassabis D. Highly accurate protein structure prediction with AlphaFold. Nature 2021; 596: 583-589.
[26] Varadi M, Bertoni D, Magana P, Paramval U, Pidruchna I, Radhakrishnan M, Tsenkov M, Nair S, Mirdita M, Yeo J, Kovalevskiy O, Tunyasuvunakool K, Laydon A, Žídek A, Tomlinson H, Hariharan D, Abrahamson J, Green T, Jumper J, Birney E, Steinegger M, Hassabis D and Velankar S. AlphaFold Protein Structure Database in 2024: providing structure coverage for over 214 million protein sequences. Nucleic Acids Res 2024; 52: D368-D375.
[27] Hybiak J, Broniarek I, Kiryczyński G, Los LD, Rosik J, Machaj F, Sławiński H, Jankowska K and Urasińska E. Aspirin and its pleiotropic application. Eur J Pharmacol 2020; 866: 172762.
[28] Vane JR. Inhibition of prostaglandin synthesis as a mechanism of action for aspirin-like drugs. Nat New Biol 1971; 231: 232-235.
[29] Dai SX, Li WX, Li GH and Huang JF. Proteome-wide prediction of targets for aspirin: new insight into the molecular mechanism of aspirin. PeerJ 2016; 4: e1791.
[30] Burton JC, Antoniades W, Okalova J, Roos MM and Grimsey NJ. Atypical p38 signaling, activation, and implications for disease. Int J Mol Sci 2021; 22: 4183.
[31] Igea A and Nebreda AR. The stress kinase p38α as a target for cancer therapy. Cancer Res 2015; 75: 3997-4002.
[32] Sahu V, Mohan A and Dey S. p38 MAP kinases: plausible diagnostic and prognostic serum protein marker of non small cell lung cancer. Exp Mol Pathol 2019; 107: 118-123.
[33] Vitos-Faleato J, Real SM, Gutierrez-Prat N, Villanueva A, Llonch E, Drosten M, Barbacid M and Nebreda AR. Requirement for epithelial p38α in KRAS-driven lung tumor progression. Proc Natl Acad Sci U S A 2020; 117: 2588-2596.
[34] Whitaker RH and Cook JG. Stress Relief Techniques: p38 MAPK determines the balance of cell cycle and apoptosis pathways. Biomolecules 2021; 11: 1444.
[35] Bi C, Zhang X, Chen Y, Dong Y, Shi Y, Lei Y, Lv D, Cao X, Li W and Shi H. MAGT1 is required for HeLa cell proliferation through regulating p21 expression, S-phase progress, and ERK/p38 MAPK MYC axis. Cell Cycle 2021; 20: 2233-2247.
[36] Shi R, Radulovich N, Ng C, Liu N, Notsuda H, Cabanero M, Martins-Filho SN, Raghavan V, Li Q, Mer AS, Rosen JC, Li M, Wang YH, Tamblyn L, Pham NA, Haibe-Kains B, Liu G, Moghal N and Tsao MS. Organoid cultures as preclinical models of non-small cell lung cancer. Clin Cancer Res 2020; 26: 1162-1174.

Supplementary Table 1. Clinical information of LG70 NSCLC tissue

Sample Name	Gender	Age	Pathological Pattern	T	N	M	EGFR mutation
LG70	Female	60	squamous cell lung carcinoma	2b	1	0	Null

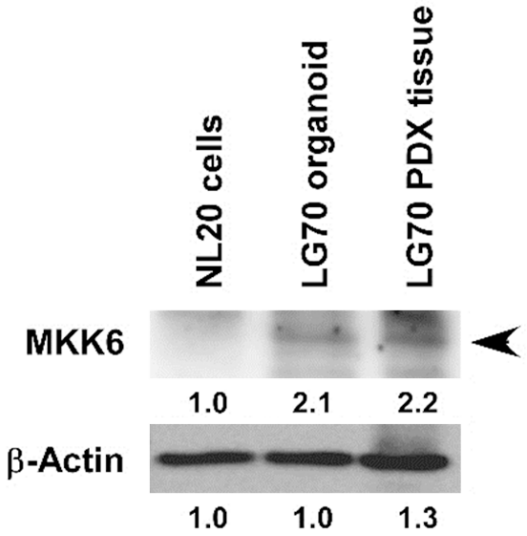

Supplementary Figure 1. The expression levels of MKK6 protein. MKK6 protein expression in human normal NL20 cells, LG70 organoid, and LG70 PDX tissue was analyzed by Western blotting. Band density was measured using the Image J (NIH) software program.